Functional Image-Guided Radiotherapy Planning in Respiratory-Gated Intensity-Modulated Radiation Therapy (IMRT) for Lung Cancer Patients with chronic obstructive pulmonary disease (COPD)

Tomoki Kimura, Ikuno Nishibuchi, Yuji Murakami, Masahiro Kenjo, Yuko Kaneyasu, Yasushi Nagata

Department of Radiation Oncology, Hiroshima University, Graduate School of Biomedical Sciences

Reprint requests to: Tomoki Kimura, Department of Radiation Oncology, Hiroshima University, Graduate School of Biomedical Sciences, 1-2-3, Kasumi, Minami-ku, Hiroshima City, 734-8551, Japan. Tel: 81-82-257-1545; Fax: 81-82-257-1546; E-mail: tkkimura@hiroshima-u.ac.jp

This work was supported in part by a Grant-in-Aid for Scientific Research from the Ministry of Education, Culture, Sports, Science and Technology of Japan (Grant no. 22591385), and a Grant-in-Aid for Scientific Research from the Association for Nuclear Technology in Medicine.

This work was partly presented at the 52nd Annual Meeting of ASTRO (American Society for Therapeutic Radiology and Oncology), San Diego, CA, USA, October 31- November 4, 2010.

Conflict of Interest Notification: none

Short running title: Functional Image-Guided Radiotherapy Planning in Respiratory- Gated IMRT for Lung Cancer

Abstract

(Purpose) To investigate the incorporation of functional lung image-derived low attenuation area (LAA) based on four-dimensional computed tomography (4D-CT) into respiratory-gated intensity-modulated radiation therapy (IMRT) or volumetric modulated arc therapy (VMAT) in treatment planning for lung cancer patients with chronic obstructive pulmonary disease (COPD)**.**

(Materials and Methods) Eight lung cancer patients with COPD were the subjects of this study. LAA was generated from 4D-CT data sets according to CT values lower than -860 Hounsfield units (HU) as a threshold. The functional lung image was defined as the area where LAA was excluded from the image of the total lung. Two respiratory-gated radiotherapy plans (70 Gy/35 fr) were designed and compared in each patient as follows: 1) Plan A: anatomical IMRT or VMAT plan based on the total lung 2) Plan F: functional IMRT or VMAT plan based on the functional lung. Dosimetric parameters (V20: the percentage of total lung volume irradiated with ≥ 20 Gy, MLD: mean dose of total lung) of the two

plans were compared.

(Results) V20 was lower in Plan F than in Plan A (mean 1.5 %, p= 0.025 in IMRT, mean 1.6 %, p= 0.044 in VMAT) achieved by a reduction in MLD (mean 0.23 Gy, p= 0.083 in IMRT, mean 0.5 Gy, p= 0.042 in VMAT). No differences were noted in target volume coverage and organ-at-risk doses.

(Conclusions) Functional image-guided radiotherapy planning based on LAA in respiratory-guided IMRT or VMAT appears to be effective in preserving a functional lung in lung cancer patients with COPD.

【Key Words】 functional imaging, 4D-CT, IMRT, COPD

INTRODUCTION

One of the most severe complications in radiation therapy for lung cancer is radiation pneumonitis (RP). Reduction of the incidence of severe RP requires a reduction of the lung dose, such as V20 which is defined as the percentage of pulmonary volume irradiated to ≥ 20 Gy. It is also one of the significant dosimetric risk factors for the incidence and severity of RP (1). Chronic obstructive pulmonary disease (COPD) is a recognized risk factor for RP (2). There has been a worldwide increase of the prevalence of COPD and as the population ages, the incidence of COPD is expected to increase (3). Pulmonary emphysema (PE) is a subtype of COPD, and defined pathologically as a group of diseases that demonstrate anatomic alterations in the lung, characterized by enlargement of airspaces distal to the terminal bronchioles, accompanied by destructive changes of alveolar walls (4). These lesions are seen as low-attenuation areas (LAAs) on CT scans, and are established findings on the imaging diagnosis of COPD (5, 6). Kimura et al reported a correlation between the incidence of RP and the extent of LAAs in the

whole lung fields (7). From these results, the functional lung image-derived LAA based on four-dimensional computed tomography (4D-CT) was developed for planning of radiation treatment to reduce the risk of RP in patients with COPD.

Several authors have described functional imaging modalities for planning of radiation treatment, such as ventilation imaging with 4D-CT (8) and single-photon emission computed tomography (SPECT) lung perfusion imaging (9). All of these authors showed that functional lung regions could be identified with imaging and then avoided with IMRT treatment planning techniques. Matsuoka (6) suggested that paired inspiratory and expiratory CT imaging can be used to define LAA volumes in patients with COPD. Therefore, these two approaches were combined in order to address the respiratory problem. This study investigated the ability of functional lung image-derived LAA based on 4D-CT, and its incorporation into respiratory-gated intensity-modulated radiation therapy (IMRT) or volumetric modulated arc therapy (VMAT) in treatment planning for lung cancer patients with COPD.

Materials and Methods

Patient background

In this study, eight male patients with lung cancer were enrolled who had undergone 4D-CT scanning and definitive radiation therapy at Hiroshima University from 2009 to 2010. Pathological diagnosis, stage (UICC 7th edition), and the primary tumor location are summarized in Table 1. All patients received [^{18}F] fluorodeoxyglucose-positron emission tomography (FDG- PET) for staging.

Functional lung image-derived LAA based on 4D-CT

At first, 4D-CT scans were acquired with 2.5-mm-thick slices using multi detector-row CT (MDCT; LightSpeed, GE Medical systems, Waukesha, WI) in cine mode with the Varian Real-time Position Management (RPM) Respiratory Gating system (Varian Medical Systems, Palo Alto, CA). Following image acquisition, the CT image data set was sorted into 10-phase bins of the respiratory cycle, and phase by phase evaluation was performed on a workstation (AdvantageSim, GE Healthcare, Princeton, NJ). The 10-phase set consisted of 0 to

90% in steps of 10 %, and 0 or 90 % was in the end-inspiratory phase and 50% in the end-expiratory phase. All 10-phase CT data sets were imported into the Eclipse treatment planning system (Varian Medical Systems, Palo Alto, CA). Several authors reported that the threshold CT value for the detection and quantification of LAA ranged from -850 to -950 HU (10, 11). Matsuoka et al concluded that the threshold of -860 HU correlated closely with airway dysfunction in COPD on paired inspiratory and expiratory CT (6). Therefore LAAs were generated from 10-phase 4D-CT data sets according to CT values lower than -860 Hounsfield units (HU) as a threshold on Eclipse.

For respiratory gated planning in this study, three expiratory phases (40-60%) were selected with the phase gating method. Fig 1 shows the three steps involved in making the functional lung image-derived LAA based on 4D-CT of case 1.

1) Acquisition of LAA at each phase (the threshold of -860HU).

2) Fusion of LAA at three expiratory phases (40-60%), and trimming the ROI as LAA image (40-60%).

3) The functional lung image was defined as the area where LAA image (40-60%) was excluded from fusion images of the total lung volumes on each of the 40-60% phases.

This technique did not employ any sort of deformable image registration algorithm in any of the steps.

Respiratory Gated IMRT and VMAT planning with functional lung image

In this simulation study, two respiratory-gated radiotherapy plans were designed and compared for each patient as follows: 1) Plan A: anatomical IMRT or VMAT plan based on the total lung; 2) Plan F: functional IMRT or VMAT plan based on the functional lung. RapidArc (Varian Medical Systems, Palo Alto, CA) was used as VMAT. In this study, IMRT was defined as fixed, non-rotational IMRT, and VMAT was defined as rotational IMRT. All dose calculations were done on the full expiration (50%) phase.

For target delineation of each plan, a physician delineated the target volume on each 10-phase CT image. Gross tumor volume (GTV) included the primary tumor

and metastatic lymph nodes, and clinical target volume (CTV) margin of 3-5 mm was added to GTV according to the pathology. Elective nodal irradiation was omitted (so-called “involved-field”). Internal target volume (ITV) was defined as the sum of CTV at three expiratory phases (40-60%) in this respiratory gated planning. A planning target volume (PTV) margin of 5-10 mm was added allowing for reproducibility of respiratory motion and setup error to ITV.

The IMRT plans consisted of five coplanar fixed beams with gantry angles of 20°, 320°, 240°, 180°, and 135° at the right lung, and 340°, 40°, 120°, 180°, and 215° at the left lung. The VMAT plans consisted of two coplanar arcs with gantry angles were moved 220° from 180° to 40° in the right lung, and from 180° to 320° in the left lung in clockwise and counter clockwise directions. Treatment plans were delivered using 6-MV photons generated by a linear accelerator (Clinac iX, Varian Medical Systems, Palo Alto, CA) with continuous changes in the gantry speed, multi-leaf collimator position, and dose rate. The collimator angle was fixed at 45° throughout the arc. The same beam arrangements were used for both plans.

A total dose of 70 Gy in 35 fractions to 95% of the PTV was prescribed. The prescribed dose was calculated with a heterogeneous dose calculation algorithm (the Eclipse anisotropic analytical algorithm; AAA). Table 2 shows the dose constraints for each structure. The constraints on the total lung were used in Plan A, and those on the two functional lung regions were used in Plan F. V20 or functional V20 (fV20) was calculated by lung-PTV and its dose constraints were defined as less than 10-30%. Therefore the background of patients included all stages. The minimal value of V20 which could be achieved in the anatomical plan of each patient was selected according to the field size of each patient, and the value of fV20 was also the same. Several IMRT and VMAT plans were made to maintain clinical acceptability, and the plans which most suitably satisfied the dose constraints in Table 2 were selected for Plans A and F.

Data analysis and Statistical methods

The dosimetric parameters of Plans A and F using respiratory guided IMRT and VMAT planning were evaluated by examining the following:

1) Lung V5-30 and fV5-30: the percentage of total or functional lung volumes irradiated with ≥5-30 Gy

2) Lung MLD and functional MLD (fMLD): mean dose to total or functional lung

3) Mean dose, homogeneity index (HI), and conformity index (CI) of PTV

   HI = maximum dose of PTV / minimum dose to PTV

   CI = Treated Volume / PTV; it is implied that Treated Volume completely encompasses the PTV

4) Mean or maximum dose of organ-at-risk (heart, esophagus, and spinal cord)

5) Monitor units of each plan

For comparison of statistical significance the Mantel-Haenzel χ^2 or t tests were used. All statistical analysis was performed using StatMate for Windows (StatMate ver 4.01; ATMS, Tokyo, Japan). Statistical significance was defined as $p<0.05$.

Results

Details of target characteristics

The details of target characteristics used in both plans are presented in Table 3.

Comparison of dosimetric parameters for lung

Figs 2A and B show the mean percentage volumes of total lung (A) or functional lung (B) receiving ≧5, ≧10, ≧20 and ≧30 Gy (V5, V10, V20, V30, and fV5, fV10, fV20, fV30, respectively) for both IMRT and VMAT. Compared with Plan A, Plan F reduced V20 in IMRT (mean 1.5 %, p= 0.025), in VMAT (mean 1.6 %, p= 0.044), V30 in IMRT (mean 1.0 %, p= 0.026), in VMAT (mean 1.3 %, p= 0.048) and fV30 in IMRT (mean 1.3 %, p= 0.048). Small reductions were noted in MLD (mean 0.23 Gy, p= 0.083 in IMRT, mean 0.5 Gy, p= 0.042 in VMAT) and fMLD (mean 0.3 Gy, p= 0.106 in IMRT, mean 0.5 Gy, p= 0.092 in VMAT).

On the other hand, compared with IMRT, VMAT reduced fV20 in Plan A (mean 2.0 %, p=0.027), and in Plan F (mean 1.3%, p=0.027), but increased V5 in Plan A (mean 16.4 %, p=0.027), in Plan F (mean 15.1%, p=0.005); V10 in Plan A (mean 8.4 %, p=0.021), in Plan F (mean 7.7 %, p=0.040); fV5 in Plan A (mean 19.0 %, p=0.001), in Plan F (mean 18.7 %, p=0.001) and fV10 in Plan A (mean 9.3 %,

p=0.025), in Plan F (mean 8.4 %, p=0.045). Significant increases were also seen in MLD (mean 1.1 Gy, p= 0.013 in Plan A, mean 0.8 Gy, p= 0.010 in Plan F) and fMLD (mean 1.1 Gy, p= 0.037 in Plan A, mean 0.9 Gy, p= 0.002 in Plan F).

Fig 3 shows V5 and fV5 in IMRT and VMAT of Plan F according to PTV. Compared with PTV < 250 cc, IMRT and VMAT significantly increased V5 and fV20 in PTV ≥ 250 cc. Additionally, compared with IMRT, VMAT also increased V5 and fV5 in PTV ≥ 250 cc significantly (P=0.0096 in V5, p= 0.0032 in fV5).

Comparison of dosimetric parameters for PTV and organ-at-risk

Table 4 (A) shows the dosimetric parameters for PTV, organ-at-risk and monitor units (MU) between Plans A and F. There were no differences of PTV mean dose, HI, CI, mean or maximum dose to organ-at-risk, such as heart, esophagus and spinal cord and MU between Plans A and F in both IMRT and VMAT.

Table 4 (B) shows the dosimetric parameters for PTV, organ-at-risk and MU between IMRT and VMAT. Compared with IMRT, VMAT improved HI and CI of PTV, especially in Plan F (p=0.040) without change in mean dose to PTV. However,

there was no difference in mean or maximum doses to heart and spinal cord between IMRT and VMAT, and VMAT increased mean dose to esophagus (mean 3.9 Gy, p=0.002 in Plan A, mean 3.6 Gy, p=0.003 in Plan F) in both Plans A and F. However, IMRT resulted in greater MU than in VMAT in both Plans A and F (p=0.008 and 0.003).

Fig 4 shows dose distribution of case 4.

Discussion

This study showed that planning of functional image-guided radiotherapy based on LAA can improve the dosimetric parameters for lung without a major change of PTV coverage and increasing other organ-at-risk doses. IMRT appears to be a good treatment planning based on favorable outcomes and in maintaining dosimetric predictors of toxicity at acceptable levels for patients who have larger tumors with difficult geometry in critical locations (12). However, in as much as reductions in MLD, V20 and V10 have been shown by IMRT, it can also increase the volume of

lung receiving low doses, such as V5, which may potentially increase lung toxicity (13, 14). For delivering safe IMRT for lung cancer, it is important for dosimetric factors to be carefully considered. In fact, severe radiation pneumonitis may be easily induced by a lower dose in patients with COPD, which is seldom comprised of normal lung tissue (7). It is especially in these patients that the functional IMRT described here may contribute to minimize the effect of lower doses.

Several authors have reported on functional imaging modalities for planning of radiation treatment. Ventilation imaging is one of the modalities, which is generated from CT image volumes of the thorax representing exhale and inhale phases obtained from components of the 4D-CT sets using a deformable image registration algorithm (8, 15). Yaremko et al reported generation of high functional regions, comprised of 90 percentile functional volume, and constituting 10 % of the lung volume where the highest ventilation occurred. IMRT plans were generated using constraints on the high functional regions. This method led to the result in which the mean dose to the high functional region was reduced by 2.9 Gy (8). Yamamoto et al

also reported the effectiveness of the ventilation imaging-based functional planning (15). In their study, functional lung was divided into high-, moderate- and low-functional regions, and the average reductions of the mean dose in the high-functional lung were 1.8 Gy for IMRT and 2.0 Gy for VMAT. This was achieved by using constraints on each region, for patients who had high-function lungs adjacent to the PTV.

SPECT lung perfusion imaging is the other functional imaging modality, which provides information about the function of pulmonary vascular and alveolar subunits. Shioyama et al reported that the functional plans reduced the median dose of the 50- and 90-percentile hyperperfusion lung to 2.2 and 4.2 Gy, respectively, compared with anatomic plans by incorporating perfusion information in IMRT planning (9).

An advantage of these modalities is that several degrees of functional regions can be described according to the degree of its regional volume change or perfusion distribution. However, the regional physiologic accuracy has not been validated in

the ventilation imaging because of the uncertainty regarding the use of deformable image registration. Additionally, the use of SPECT lung perfusion imaging is limited by the need for separate imaging sessions or fusions in radiotherapy planning.

The functional lung image-derived LAA based on 4D-CT of this study focused only on describing non-functional lung regions. The advantages of this method are: 1) Actual lung function may be easily recognized especially in patients with COPD by using LAA-based images. 2) Our LAA approach can be done simply, without the need of a sophisticated deformable image registration algorithm. 3) This method may be less affected by respiratory motion because of the respiratory-gated technique. Consequently, there was limited description of several degrees of functional regions. However, CT quantitation using LAA is already an established tool for in vivo assessment of COPD, and has been correlated with pulmonary function (10, 11). Especially in CT findings of patients with COPD, LAA appears as areas of decreased lung attenuation due to an air-trapping phenomenon, which is

characterized by progressive air way obstruction and airflow limitation that are not reversible with the administration of bronchodilator drugs (16). Therefore Zaporozhan et al reported that PE volumes measured from expiratory MDCT scans better reflect abnormalities in pulmonary function tests in patients with severe PE than in those from inspiratory scans (17). Considering the better reproducibility of lung motion, expiratory phases of 4D-CT were selected for this study. A problem remains in that 4D-CT data acquisition by this method is affected by respiratory motion. Thus, the proper thresholds of CT values for the detection and quantification of LAA and the correlations with pulmonary function using this method need to be evaluated. Nevertheless, the advantage of this respiratory gated method is that it can reduce not only the artifact of respiratory motion but also the total lung dose to a minimum.

Fixed-beam IMRT and VMAT plans were also compared. An advantage of VMAT over IMRT is the improvement of target conformity and the potential reduction in delivery time, especially in stereotactic body radiotherapy for lung

cancer which requires a large number of beams and monitor units (18). On the other hand, Schallenkamp et al reported that larger volumes of lungs treated with lower doses may be more critical in predicting adverse events than smaller volumes treated with higher doses, especially when using the IMRT technique which delivers low doses of radiation to large lung volumes (19). Yamamoto et al reported that functional IMRT and VMAT planning had a similar impact on each other for high-functional lung dose, PTV metrics, and doses to other critical organs (15). In our comparison with IMRT, although VMAT reduced fV20 and MU and improved HI and CI of PTV, VMAT increased the low dose areas in both plans, especially in patients with large PTV. Increasing the low dose area of lung using VMAT in patients with large PTV needs to be approached with caution.

The use of functional lung image-derived LAA into respiratory-gated IMRT or VMAT in planning for lung cancer patients may remove the uncertainties of quantifying LAA due to respiratory motion, and result in further reductions of total and functional lung doses in functional planning. However, several problems need

to be addressed for clinical use. Prospective clinical trials will be necessary to determine whether treatment results, such as survival and complications, are improved by using this functional avoidance treatment planning.

Conclusions

In conclusion, functional image-guided radiotherapy planning based on LAA in respiratory-guided IMRT or VMAT appears to be effective in preserving a functional lung in lung cancer patients with COPD. Further investigations are needed, including those to clarify several technical problems mentioned above, and to conduct prospective clinical trials.

REFERENCES

1. Graham MV, Purdy JA, Emami B, et al. Clinical dose-volume histogram analysis for pneumonitis after 3D treatment for non-small cell lung cancer

(NSCLC). Int J Radiat Oncol Biol Phys 1999; 45: 323-329.

2. Rancati T, Ceresoli GL, Gagliardi G, et al. Factors predicting radiation pneumonitis in lung cancer patients: a retrospective study. Radiother Oncol 2003; 67 : 275-283.

3. Fukuchi Y, Nishimura M, Ichinose M, et al. COPD in Japan: the Nippon COPD Epidemiology study. Respirology 2004; 9: 458-463.

4. American Thoracic Society. Standard for the diagnosis and care of patients with chronic obstructive pulmonary disease (COPD) and asthma. *Am Rev Respir Dis* 1987; 136: 225–232.

5. Orlandi I, Moroni C, Camiciottoli G, et al. Chronic obstructive pulmonary disease: Thin-section CT measurement of airway wall thickness and lung attenuation. Radiology 2005; 234: 604-610.

6. Matsuoka S, Kurihara Y, Yagihashi K, et al. Quantitative assessment of air trapping in chronic obstructive pulmonary disease using inspiratory and expiratory volumetric MDCT. AJR 2008; 190: 762-769.

7. Kimura T, Togami T, Takashima H, et al. Radiation Pneumonitis in Patients with Lung and Mediastinal Tumors: A retrospective study of risk factors focused on pulmonary emphysema. British J. Radiol In press.

8. Yaremko BP, Guerrero TM, Noyola-Martinez J, et al. Reduction of normal lung irradiation in locally advanced non-small cell lung cancer patients, using ventilation images for functional avoidance. Int J Radiat Oncol Biol Phys 2007; 68: 562-571.

9. Shioyama Y, Jang SY, Liu HH, et al. Preserving functional lung using perfusion imaging and intensity-modulated radiation therapy for advanced-stage non-small cell lung cancer. Int J Radiat Oncol Biol Phys 2006; 68: 562-571.

10. Park KJ, Bergin CJ and Clausen JL. Quantitation of emphysema with three-dimensional CT densitometry: Comparison with two-dimensional analysis, visual emphysema scores, and pulmonary function test results. Radiology 1999; 211: 541-547/

11. Gevenois PA, Vuyst PD, Sy M, et al. Pulmonary emphysema: Quantitative CT

during expiration. Radiology 1996; 1999: 825-829.

12. Sura S, Gupta V, Yorke E, et al. Intensity-modulated radiation therapy (IMRT) for inoperable non-small cell lung cancer: The Memorial Sloan-Kettering Cancer Center (MSKCC) experience. Radiother and Oncol 2008; 87: 17-23.

13. Liu HH, Wang X, Dong L, et al. Feasibility of sparing lung and other thoracic structures with intensity-modulated radiotherapy for non-small cell lung cancer. Int J Radiat Oncol Biol Phys 2004; 58: 1268-1279.

14. Murshed H, Liu HH, Liao Z, et al. Dose and volume reduction for normal lung using intensity-modulated radiotherapy for advanced-stage non-small cell lung cancer. Int J Radiat Oncol Biol Phys 2004; 58: 1257-1267.

15. Yamamoto T, Kabus S, Berg JV, et al. Impact of four-dimensional computed tomography pulmonary ventilation imaging-based functional avoidance for lung cancer radiotherapy. Int J Radiat Oncol Biol Phys 2011; 79: 279-288.

16. American Thoracic Society. Standards for the diagnosis and care of patients with chronic obstructive pulmonary disease. Am J Respir Crit Care Med 1995;

152: S77-83.

17. Zaporozham J, Ley S, Eberhardt R, et al. Paired inspiratory/expiratory volumetric thin-slice CT scans for emphysema analysis. Chest 2005; 128: 3212-3220.

18. Matuszak MM, Yan D, Grills I, et al. Clinical applications of volumetric modulated arc therapy. Int J Radiat Oncol Biol Phys 2010; 77: 608-616.

19. Schallenkamp JM, Miller RC, Brinkmann DH, et al. Incidence of radiation pneumonitis after thoracic irradiation: Dose-volume correlates. Int J Radiat Oncol Biol Phys 2007; 67: 410-416.

Figure legends

[Fig 1] Fig 1 shows three steps to make the functional lung image-derived low attenuation area (LAA) based on four-dimensional computed tomography (4D-CT) of case 1.

[Fig 2] Comparison of V5-30 and fV5-30 in Plan A and F using IMRT and VMAT

(mean ± SD). The p-values shown are only for statistically significant differences

[Fig 3] Comparison of V5 and fV5 in IMRT and VMAT of Plan F according to PTV. The p-values shown are only for statistically significant differences

[Fig 4] Dose distribution of case 4.

(A) IMRT plan A, (B) IMRT plan F, (C) VMAT plan A, and (D) VMAT plan F show isodose line ≧20 Gy (blue) and functional lung area (green). The isodose line ≥20 Gy was decreased at the functional lung in VMAT Plan F (red arrows).

Table 1. Patients' Background

case	age	gender	histology	TNM	stage	tumor location
1	81	M	non-small	T2aN1M0	IIB	R.S8
2	86	M	SCC	T2aN0M0	IB	L.S8
3	56	M	adeno	T4N2M0	IIIB	R.S1
4	68	M	small	T2aN1M0	IIB	R.S10
5	71	M	SCC	T2aN3M0	IIIB	R.S10
6	74	M	small	T2aN2M0	IIIA	L.S8
7	68	M	SCC	T3N2M0	IIIA	R.S6
8	84	M	non-small	T1N0M0	IA	L.S8

Table 2. Dose constraints for IMRT and VMAT

		Plan A: anatomical plan			Plan F: functional plan		
		volume (%)	**Dose (cGy)**	**Priority**	**volume (%)**	**Dose (cGy)**	**Priority**
PTV	upper	0	7350	70	0	7350	70
		10	7200	70	10	7200	70
	lower	98	7000	80	98	7000	80
		100	6650	70	100	6650	70
cord	upper	0	4500	90	0	4500	90
esophagus	upper	0	7350	50	0	7350	50
		35	5500	50	35	5500	50
heart	upper	50	4500	50	50	4500	50
body	upper	0	7500	50	0	7500	50
lung	upper	10~30	2000	90			
f-lung[#]	upper				10~30	2000	120
low f-lung (LAA[$]**)**	upper				10~30	2000	90

#: functional lung

$: low atenuation area

Table 3. Details of Target (PTV), Normal Tissue and Dosimetric Characteristics

case	PTV (cm^3)	Total lung volume (cm^3)	Functional lung volume (cm^3)	Defect size (as % of total lung)	Dose constraints of V20 or fV20
1	158.8	3354.5	1617.6	51.8	<20%
2	228.3	2819.6	1717.3	39.1	<10%
3	207.3	3258.1	2302.3	29.3	<10%
4	278.4	2719.1	2012.5	26	<30%
5	505.9	2490	2264.1	9.1	<20%
6	256.4	2885.4	1586.6	45	<25%
7	561.1	2517.1	1903.4	24.4	<25%
8	62.4	3124.2	866.8	72.3	<10%
mean	282.3	2896	1810.4	37.1	

Table 4. Comparison of dosimetric parameters of PTV and normal tissue between anatomical and functional plans, for IMRT and VMAT (mean ± SD)

(A)		IMRT			VMAT		
		Anatomical	Functional	p-value	Anatomical	Functional	p-value
PTV	mean dose (Gy)	72.6 ± 1.2	72.9 ± 0.9	0.155	72.2 ± 1.0	72.3 ± 1.1	0.629
	Homogeneity index[#]	1.52 ± 0.08	1.59 ± 0.08	0.056	1.51 ± 0.10	1.51 ± 0.10	1
	Conformity index[$]	2.74 ± 0.72	3.17 ± 1.07	0.128	2.44 ± 0.49	2.53 ± 0.49	0.356
Heart	mean dose (Gy)	19.7 ± 9.7	20.6 ± 10.6	0.214	19.1 ± 10.2	19.9 ± 11.1	0.356
Esophagus	mean dose (Gy)	15.6 ± 11.4	15.6 ± 11.6	0.951	19.5 ± 13.1	19.2 ± 13.2	0.522
Spinal cord	mean dose (Gy)	9.1 ± 6.3	9.2 ± 6.3	0.456	10.3 ± 5.4	9.9 ± 5.8	0.257
	maximum dose (Gy)	40.6 ± 21.2	40.6 ± 20.5	0.954	42.0 ± 14.6	41.1 ± 15.9	0.269
MU		786.8± 214.3	817.3± 203.1	0.378	496.5± 60.9	529.9± 56.5	0.149

(B)		Anatomical			Functional		
		IMRT	VMAT	p-value	IMRT	VMAT	p-value
PTV	mean dose (Gy)	72.6 ± 1.2	72.2 ± 1.0	0.275	72.9 ± 0.9	72.3 ± 1.1	0.129
	Homogeneity index[#]	1.52 ± 0.08	1.51 ± 0.10	0.831	1.59 ± 0.08	1.51 ± 0.10	0.077
	Conformity index[$]	2.74 ± 0.72	2.44 ± 0.49	0.23	3.17 ± 1.07	2.53 ± 0.49	0.04
Heart	mean dose (Gy)	19.7 ± 9.7	19.1 ± 10.2	0.639	20.6 ± 10.6	19.9 ± 11.1	0.671
Esophagus	mean dose (Gy)	15.6 ± 11.4	19.5 ± 13.1	0.002	15.6 ± 11.6	19.2 ± 13.2	0.003
Spinal cord	mean dose (Gy)	9.1 ± 6.3	10.3 ± 5.4	0.117	9.2 ± 6.3	9.9 ± 5.8	0.281
	maximum dose (Gy)	40.6 ± 21.2	42.0 ± 14.6	0.711	40.6 ± 20.5	41.1 ± 15.9	0.888
MU		786.8± 214.3	496.5± 60.9	0.008	817.3± 203.1	529.9± 56.5	0.003

#: maximum dose of PTV / minimum dose of PTV

$: irradiated volume which is covered by minimum dose of PTV / PTV

Fig. 1

1) Acquisition of LAA at each phase
(the threshold of -860HU)

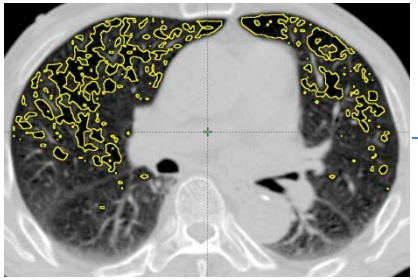

LAA (40% phase)

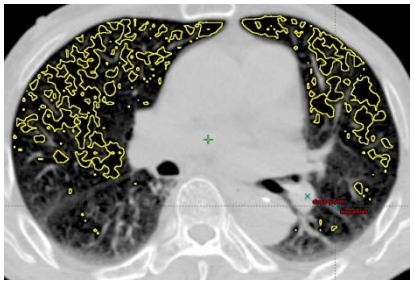

LAA (50% phase)

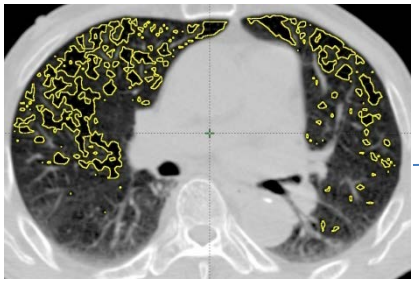

LAA (60% phase)

2) Fusion of LAA at 40-60% phase
and trimming the ROI

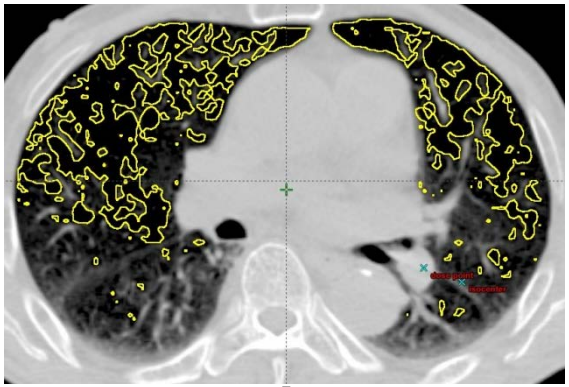

trimming

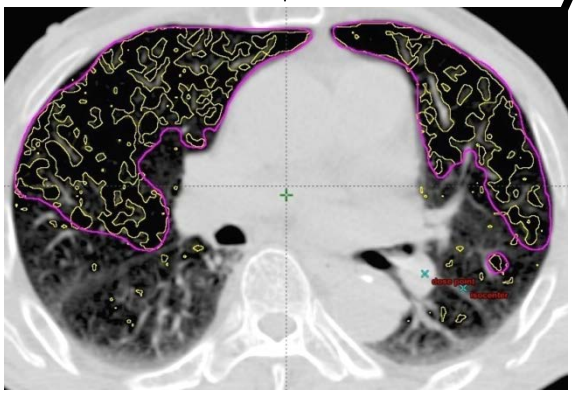

LAA image (40-60% phase)

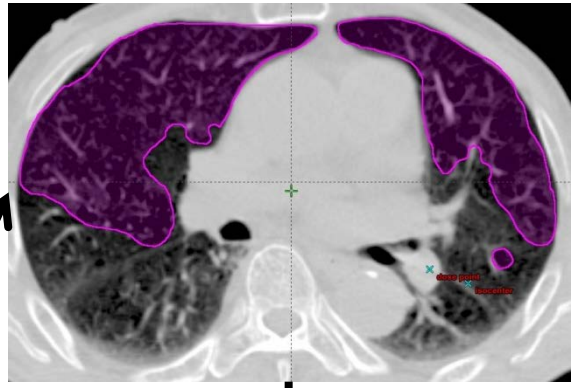

3) LAA image (40-60% phase) is
excluded from total lung volume

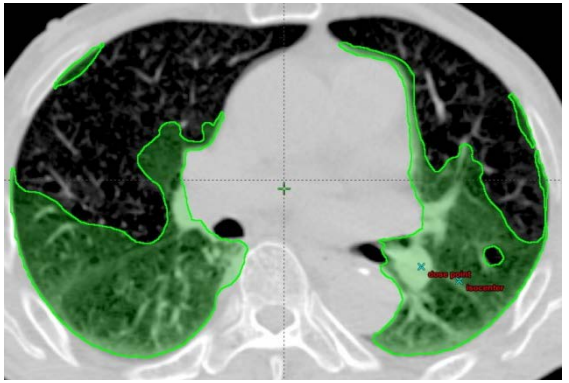

Functional lung (40-60% phase)

Fig. 2 (A)

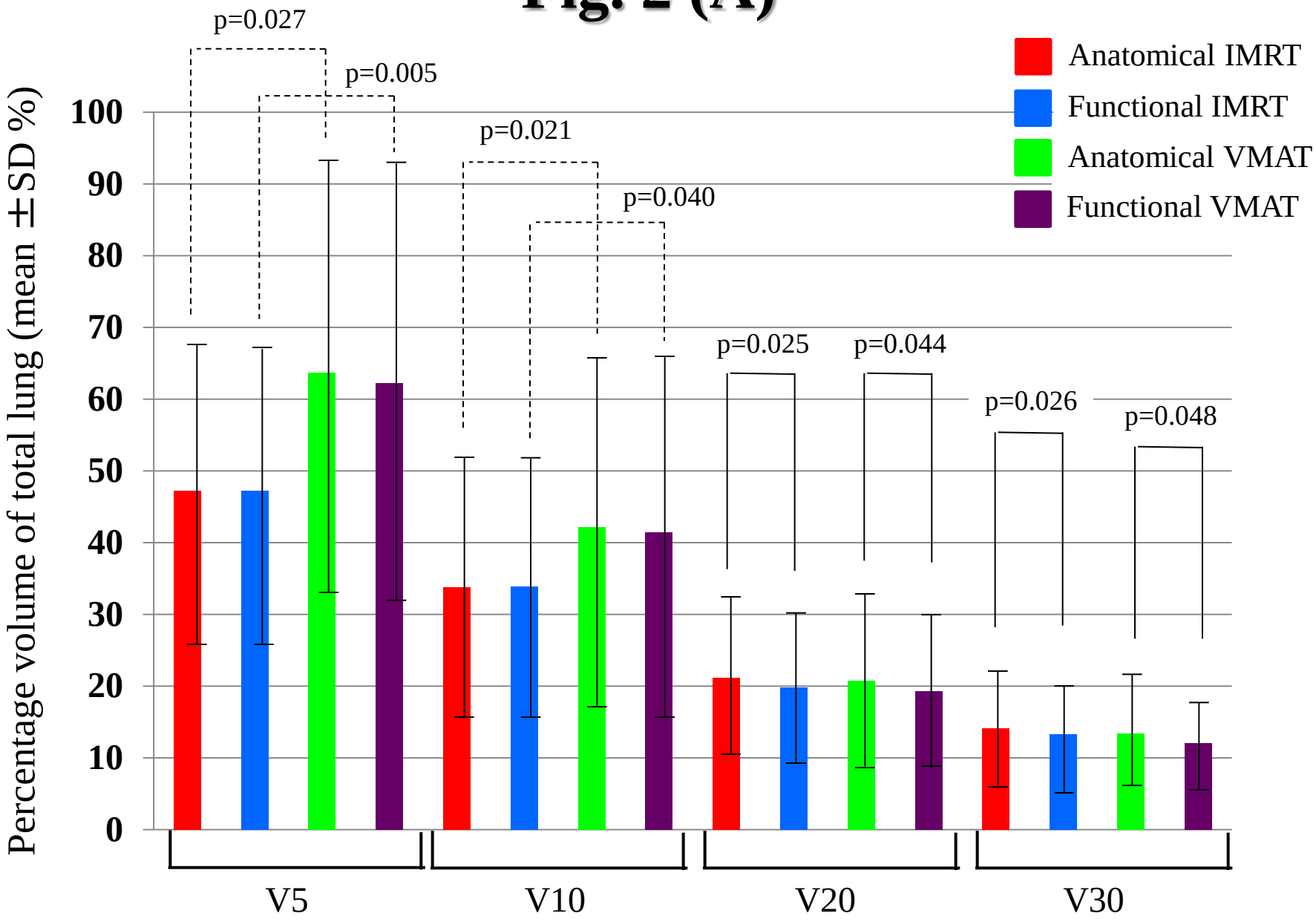
p=0.027
p=0.005
p=0.021
p=0.040
p=0.025
p=0.044
p=0.026
p=0.048
Anatomical IMRT
Functional IMRT
Anatomical VMAT
Functional VMAT
Percentage volume of total lung (mean ± SD %)
100
90
80
70
60
50
40
30
20
10
0
V5
V10
V20
V30

Fig. 2 (B)

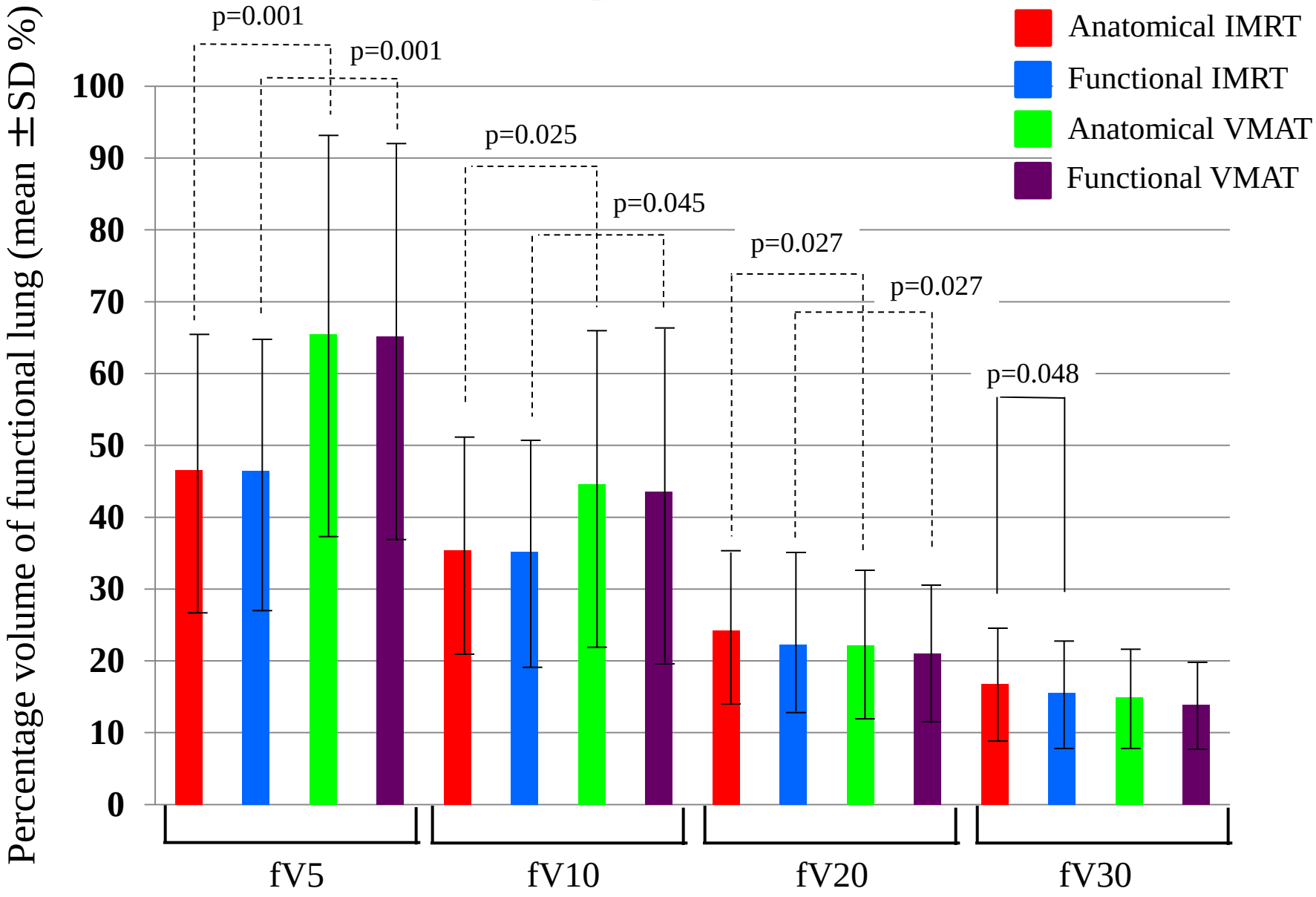
Percentage volume of functional lung (mean ± SD %)
100
90
80
70
60
50
40
30
20
10
0
p=0.001
p=0.001
p=0.025
p=0.045
p=0.027
p=0.027
p=0.048
Anatomical IMRT
Functional IMRT
Anatomical VMAT
Functional VMAT
fV5
fV10
fV20
fV30

Fig. 3

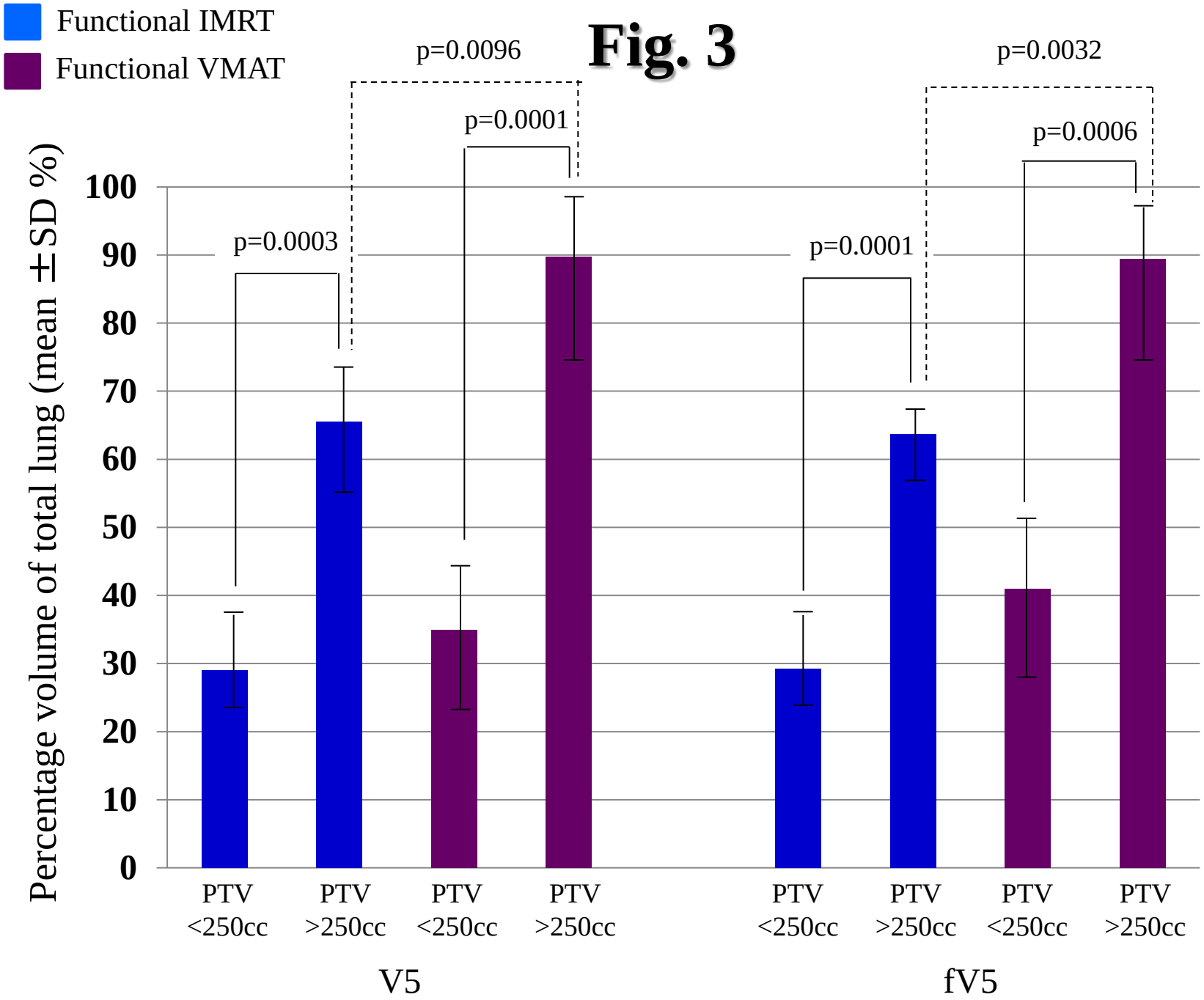
Functional IMRT
Functional VMAT
Percentage volume of total lung (mean ±SD %)
100
90
80
70
60
50
40
30
20
10
0
p=0.0096
p=0.0001
p=0.0003
p=0.0032
p=0.0006
p=0.0001
PTV <250cc
PTV >250cc
PTV <250cc
PTV >250cc
PTV <250cc
PTV >250cc
PTV <250cc
PTV >250cc
V5
fV5

Fig. 4 (A-D)

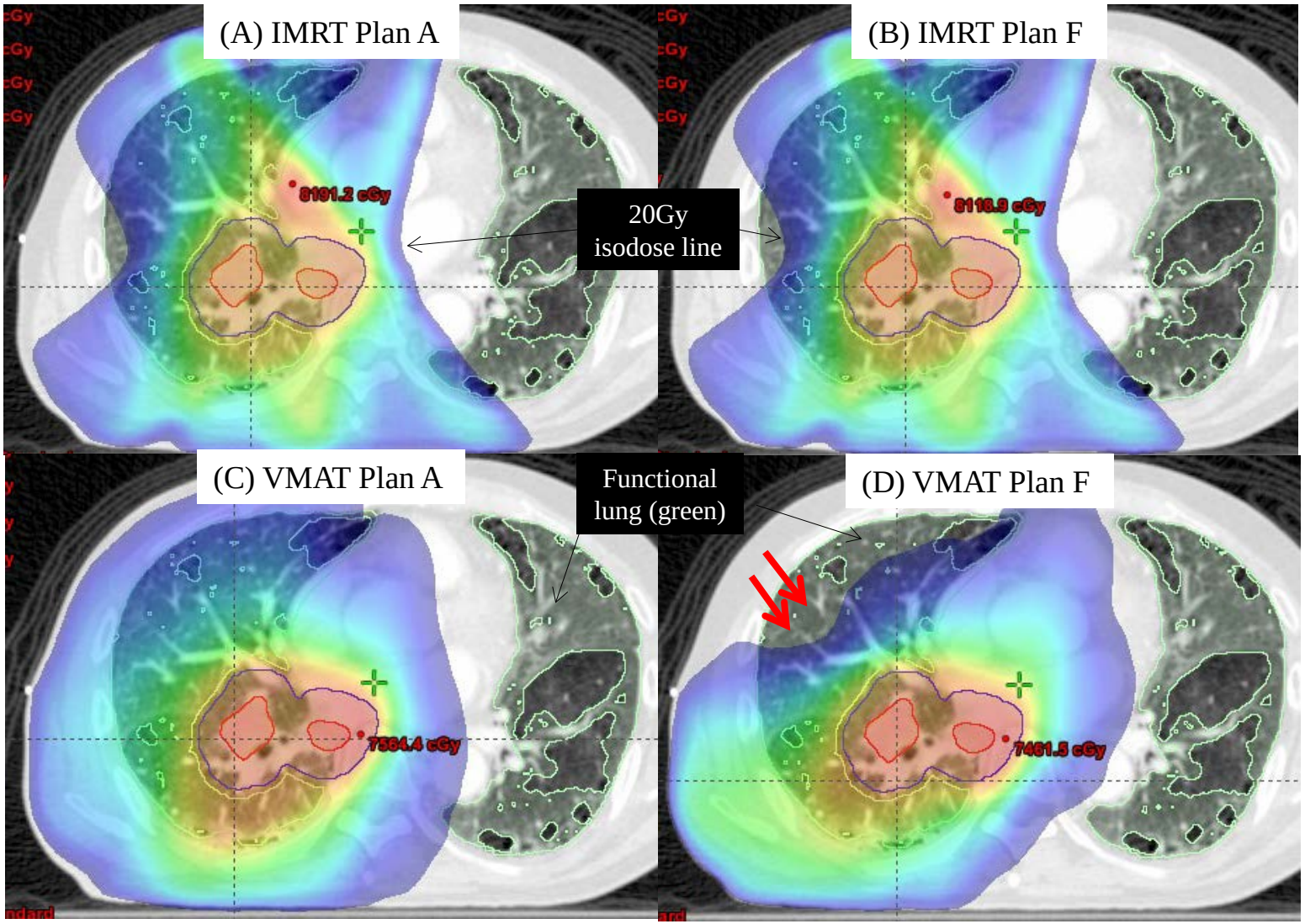
(A) IMRT Plan A
(B) IMRT Plan F
20Gy
isodose line
(C) VMAT Plan A
Functional
lung (green)
(D) VMAT Plan F